Global Journal of Science Frontier Research: H
Environment & Earth Science
Volume 20 Issue 4 Version 1.0 Year 2020
Type: Double Blind Peer Reviewed International Research Journal
Publisher: Global Journals
Online ISSN:2249-4626 & Print ISSN:0975-5896

Estimation of Hurricane Intensity from ATMS-Derived Temperature Anomaly using Machine Learning

By Lin Lin
ESSIC/University of Maryland

Abstract- The warm-core structure is one of the basic characteristics that vary during the different stages of tropical cyclones (TCs). The warm core structure of the TCs during 2016-2019 over the Atlantic Ocean was derived based on the observations of the ATMS onboard S-NPP. From linear regression, the mean prediction error (MPE) is 39.04 mph for V_{max} and 14.47 hPa for P_{min}. The root-mean-square error (RMSE) is 42.70 mph for the maximum sustained wind (V_{max}) and 77.69 hPa for the minimum sea-level pressure (P_{min}). Several machine learning (ML) techniques are used to develop the Atlantic TC intensity (V_{max} and P_{min}) estimation models. The support vector machine (SVM) model has the best performance with the MPE of 14.62 mph for V_{max} an 7.66 hPa for P_{min}, and the RMSE of 19.91 mph for V_{max} and 10.58 hPa for P_{min}. Adding latitude and day of year (DOY) can further improve the estimation of V_{max} by decreasing MPE to 13.01 mph and RME to 17.33 mph using SVM. Best estimation of P_{min} occurs when adding the day of year to the training process, as the MPE is 7.23 hPa and RMS is 9.88 hPa. Other TC information, such as longitude and local time, does not help to improve the performance of the hurricane intensity estimation models significantly.

Keywords: ATMS, warm core, atlantic hurricane intensity, machine learning.

GJSFR-H Classification: FOR Code: 059999p

EstimationofHurricaneIntensityfromATMSDerivedTemperatureAno

Strictly as per the compliance and regulations of:

Estimation of Hurricane Intensity from ATMS-Derived Temperature Anomaly using Machine Learning

Lin Lin

Abstract- **The warm-core structure is one of the basic characteristics that vary during the different stages of tropical cyclones (TCs). The warm core structure of the TCs during 2016-2019 over the Atlantic Ocean was derived based on the observations of the ATMS onboard S-NPP. From linear regression, the mean prediction error (MPE) is 39.04 mph for V_{max} and 14.47 hPa for P_{min}. The root-mean-square error (RMSE) is 42.70 mph for the maximum sustained wind (V_{max}) and 77.69 hPa for the minimum sea-level pressure (P_{min}). Several machine learning (ML) techniques are used to develop the Atlantic TC intensity (V_{max} and P_{min}) estimation models. The support vector machine (SVM) model has the best performance with the MPE of 14.62 mph for V_{max} an 7.66 hPa for P_{min}, and the RMSE of 19.91 mph for V_{max} and 10.58 hPa for P_{min}. Adding latitude and day of year (DOY) can further improve the estimation of V_{max} by decreasing MPE to 13.01 mph and RME to 17.33 mph using SVM. Best estimation of P_{min} occurs when adding the day of year to the training process, as the MPE is 7.23 hPa and RMS is 9.88 hPa. Other TC information, such as longitude and local time, does not help to improve the performance of the hurricane intensity estimation models significantly.**

Key Points

- ATMS-derived maximum temperature anomalies in hurricanes are highly correlated with the hurricane intensities over the Atlantic Ocean.
- Compared with linear regression, machine learning can estimate hurricane intensity more accurately.

Keywords: ATMS, warm core, atlantic hurricane intensity, machine learning.

I. Introduction

The intensity of a tropical cyclone (TC) is defined as the maximum 1-minute surface wind near the center of the TC. Accurate estimation of it is necessary for early warning/management of disasters. Moreover, accurate estimation of TC intensity can benefit better initialization of the hurricane forecasting models, which can help to improve the hurricane forecasting.

Most of TC's life is spent over open oceans. A major problem with TC intensity estimation and prediction is the lack of in-situ observations because there are very few surface observations on small islands and from buoys. Although supplementary data can be obtained from reconnaissance, i.e., research aircraft with radar, radiosondes, and other instruments, such missions are costly and limited to the Atlantic Ocean and the eastern North Pacific Ocean. Satellite remote sensing observations cannot directly measure surface winds, they can provide high temporal resolution data from over the globe (e.g., clouds, water vapor, and precipitation) from combined Polar and Geostationary platforms to help estimate the TC intensity.

Microwave instruments have a long history of describing TCs because of their advantages, namely, that microwave radiation can penetrate clouds and that microwave radiation is sensitive to a variety of atmospheric parameters, including temperature, moisture, cloud liquid water, and cloud ice water. Since the 1960s and 1970s, a warm temperature anomaly has been observed in the hurricane atmosphere from microwave sounders, such as the Microwave Sounding Unit (MSU), the Advanced Microwave Sounding (AMSU), and the Advanced Technology Microwave Sounder (ATMS) (Kidder et al., 1978, 1980; Velden and Smith, 1983; Velden, 1989; Velden et al., 1991; Kidder et al., 2000; Zhu and Weng, 2013; Lin and Weng, 2018), and also from aircraft field campaigns and Global Positioning System dropsonde observations (La Seur and Hawkins, 1963; Hawkins and Rubsam, 1968; Hawkins and Imbembo, 1976; Halverson et al., 2006; Dolling and Barnes, 2014; Stern and Zhang, 2016; Brown et al., 2017). Two methods are usually used to retrieve the thermal structure of TCs from satellite microwave sounding data, i.e., statistical algorithms (Goldberg, 1999; Kidder et al., 2000; Zhu et al., 2002; Zhu and Weng, 2013; Tian and Zou, 2016; Lin and Weng, 2018), and one-dimensional variation algorithms (1DVAR) (Han and Weng, 2018; Hu and Weng, 2019).

A typical hurricane is accompanied by a warm core anomaly that can cause the brightness temperature (T_b) of the sounding channel at high altitude to increase by a few degrees. Moreover, characteristics of the warm core are closely related to changes of TC intensity (Wang et al., 2010; Dolling and Barnes, 2012; Zhang and Chen, 2012; Galarneau et al. 2013; Zhu and Weng, 2013; Lin and Weng, 2018; Wang and Jiang, 2019). Zhu and Weng (2013) developed a regression

Author: ESSIC/University of Maryland, College Park, MD.
e-mail: linlin@umd.edu

algorithm to retrieve atmospheric temperature using the Suomi-National Polar-orbiting Partnership (S-NPP) ATMS data. After studying ten Atlantic TCs in 2012, they concluded that the warm-core strength usually increases with TC intensity. The correlation coefficients between the maximum warm core (WC_{max}) and the maximum sustained wind (V_{max}) and the minimum sea level pressure (P_{min}) were 0.78 and -0.83, respectively. Lin and Weng (2018) used an improved temperature retrieval algorithm developed by Tian and Zou (2016) and studied the three major hurricanes (Harvey, Irma, and Maria) over the Atlantic Ocean in 2017, obtaining a correlation coefficient of 0.67 between WC_{max} and V_{max}. However, the sample sizes of these two studies are very small, and the linear relationship between WC_{max} and TC intensity is not statistically significant.

In this study, examined were TCs on the Atlantic Ocean from 2016 to 2019 using S-NPP ATMS data, and used were traditional linear regression and several machine learning (ML) schemes to analyze the relationship between WC_{max} and TC intensity (V_{max} and P_{min}). Also evaluated was the impact of introducing additional TC information into the ML schemes, i.e., latitude, longitude, local time, and day of the year (DOY), on the TC intensity estimation. This paper is organized as follows. Section 2 introduces the S-NPP ATMS data, the TC best track data, and the ATMS overpass selection. Section 3 briefly describes the ATMS atmospheric temperature retrieval algorithm and several ML techniques used in this study. Section 4 compares the performance of linear regression and ML models in the hurricane intensity (V_{max} and P_{min}) estimation. Section 5 provides a summary and conclusions.

II. Methodology

a) Warm-core retrieval algorithm for ATMS

There are several steps to obtain atmospheric temperature from a microwave sounder. First, the satellite observations (T_b) need to be corrected for antenna side lobes and limb adjustments. Then, using collocated reanalysis/radiosonde/dropsonde data, a linear regression is performed to obtain the relationship between the corrected satellite T_b and the atmospheric temperature from the surface to the Stratosphere. Goldberg (1999), Zhu and Weng (2013), Tian and Zou (2016), Zhang et al. (2017), and Lin and Weng (2018) provide more details about AMSU-A and ATMS temperature retrievals.

In this study, the atmospheric temperature is retrieved following Tian and Zou (2016). The temperature (T) at pressure level (p), with the sensor zenith angle (θ) can be obtained from a linear combination of ATMS T_b on the detection channel (v_i) as follows:

$$T(p\ \theta) = C_0(p\ \theta) + \sum_{i=i_{1,p}}^{i_{n,p}} C_i(p\ \theta) T_b(v_i, \theta) \qquad (1)$$

where $i_{1,p}, ..., i_{n,p}$ are a subset of ATMS channels 5–15 that are significantly correlated with the temperature at the pressure level p, and C_0 and C_i are the regression coefficients. In this algorithm, only ATMS channels 5–15 are selected because these channels are not affected by surface emissions and precipitation. The regression coefficients in Eq. (1) were generated for clear sky and cloudy condition separately. Pixels under clear-sky condition are defined when the cloud liquid water path (CLWP) retrieved from ATMS 23.8 GHz and 31.2 GHz channels is less than 0.015 kg/m^2 following Weng et al. (2003).

The temperature anomaly near the TC is defined as the difference between the temperatures obtained from Eq. (1) and the ambient reference temperature. Options of the reference sounding include the mean tropical sounding (La Seur and Hawkins, 1963; Hawkins and Rubsam, 1968; Hawkins and Imbembo, 1976), the domain-averaged sounding excludingthe TC (Zhu and Weng, 2013; Lin and Weng, 2018), and the average sounding in a ring space within a certain distance from the center of the TC (Knaff et al., 2004; Halverson et al. 2006). Recent research (Durden, 2013; Stern and Zhang, 2016; Munsell et al., 2018) suggests using an average of at least several hundred kilometers away from the TC center. In this study, the temperature anomaly is defined as the temperature retrieved from the ATMS minus its average temperature in the 20° latitude/longitude box but outside the cloudy area where CLWP > 0.015 kg/m^2. The strength of the warm core is defined as the highest temperature anomaly within 20 km from the TC center.

b) Machine Learning Techniques

Over the past three decades, ML, a fusion of principles from statistics and computer science, has grown tremendously and can be used in many applications. As computer power increases, ML can be used to build effective prediction models. Among the popular ML prediction models are the decision tree methods, including random forests (RFs), and the kernel methods, including support vector machines (SVM). One of the major advantages of these ML techniques is that they do not rely on the explicit assumptions required by traditional statistical models. In this study, used to develop the hurricane intensity estimation model are SVM, the multi-layer perceptron (MLP), the decision tree (DT), the Adaptive Boosting (Ada Boost), Ada Boost with DT (ADT), and the RF techniques.

The SVM is one of the most popular ML methods, successfully applied to classification, regression, and other learning tasks. In the present study, the radial basis function kernel was selected. This study also used the MLP, which is a feed-forward network consisting of an input layer, multiple hidden layers, and an output layer. A three-hidden-layer configuration was chosen because both the uncertainty and computing time are relatively low. The weights of the MLP were optimized by the Limited-memory Broyden–Fletcher–Goldfarb–Shanno solver, and the transfer (activation) function of the neurons was the hyperbolic tangent sigmoid function. DT is an analysis method that evaluates the risk of a project and determines its feasibility by constructing a decision tree based on the known probability of occurrence of various situations. It represents a mapping relationship between object attributes and object values. In this study, the number of estimators is set to 1, and the maximum depth is set to 3. AdaBoost is used in combination with DT to improve the performance by feeding into the tree growth algorithm to obtain future tree tendencies in the training sample collected at each stage of DT. The number of estimators is 300, and the maximum depth is 3. RF is a holistic learning method for classification, regression, and other tasks. It operates a tree by constructing a large number of decision trees during training and using these classes as the mean prediction (regression). In this study, the maximum depth is 3 in RF.

c) Performance Evaluation Metrics for linear regression and ML models

The model performance is then quantitatively evaluated using two statistical indicators, i.e., the mean prediction error (MPE) and the root-mean-square error (RMSE) between model estimation and the best track data. The indicators are calculated as follows:

$$\mathrm{MPE} = \frac{1}{n}\sum_{i=1}^{n}\left|y^{\mathrm{best-track}}(i) - y^{\mathrm{model}}(i)\right|, \quad (3)$$

and

$$\mathrm{RMSE} = \sqrt{\frac{1}{n}\sum_{i=1}^{n}\left(y^{\mathrm{best-track}}(i) - y^{\mathrm{model}}(i)\right)^2}, \quad (4)$$

where n is the total number of samples (=144), y is V_{max} or P_{min}, $y^{best-track}$ is the best track data, and y^{model} is the model prediction from linearregression and the ML schemes described in section 2.2.

III. Description of ATMS and Hurricane Data

a) Characteristics of ATMS Data

The ATMS is a cross-track microwave radiometer with 22 channels that can measure microwave radiances from 23.8 to 183.3 GHz. The ATMS inherits most of the sounding channels of previous instruments AMSU-A and the Microwave Humidity Sounder (MHS), which were carried by the previously launched NOAA polar-orbiting satellite. The ATMS was first deployed on the S-NPP satellite and then on the NOAA-20 satellite. S-NPP, as a pathfinder for the Joint Polar Satellite System operational satellite series in the United States, was successfully launched into a circular, near-polar, afternoon-configured orbit on 28 October 2011 (Weng et al., 2012). On 18 November 2017, the NOAA-20 satellite was also successfully launched into a sun-synchronous orbit similar to the S-NPP orbit. So far, the ATMS onboard S-NPP is still performing well.

The ATMS can provide detailed atmospheric temperature information from the surface to about 1 hPa (~45 km) and tropospheric water vapor information from the surface to about 200 hPa (~10 km) under both clear and cloudy conditions, except for heavy precipitation conditions. Compared with the AMSU-A and MHS, the ATMS can provide more detailed information on warm cores with a higher spatial resolution and a wider scan swath.

b) TC Best Track Data and Selection of ATMS Overpasses

Based on best track data from the National Hurricane Center, the intensity and location of storm centers were obtained for Atlantic TCs during 2016–2019. The TC intensity includes the 1-minute V_{max} and P_{min} at the center of the storm. All of them are linearly interpolated to match the observation time of the ATMS.

The ATMS has a band width of 1,429 km, and it is not possible for it to observe all TCs. Selected here are ATMS overpasses that can capture the TC center, resulting in a total of 721 ATMS TC overpasses in 66 TCs during 2016-2019. Among them, 577 overpasses occurred between 2016 and 2018, and 144 overpasses occurred in 2019. Overpasses were dived into seven TC intensity categories: tropical depression (TD), tropical storm (TS), category 1 (H1), category 2 (H2), category 3 (H3), category 4 (H4), and category 5 (H5) according to the Saffir-Simpson hurricane wind scale. Table 1 shows the number of ATMS overpasses for each intensity category and different latitudes over the Atlantic Ocean in 2016-2018 and 2019, respectively. Generally, as the TC intensity increases, the number of overpasses decreases, which is consistent with the statistics in the best track data. Figure 1 shows the geographic distribution of TC centers covered by the 721 selected ATMS overpasses during 2016–2018 and 2019. The strongest TCs (H4 and H5) mostly occurred between 10^o and 30^o latitudes.

Global Journal of Science Frontier Research (H) Volume XX Issue IV Version I Year 2020 7

Table 1: The number of TCs with S-NPP ATMS overpasses during 2016-2018 and 2019 individually.

	2016-2018							2019						
50-60N	TD	TS	H1	H2	H3	H4	H5	TD	TS	H1	H2	H3	H4	H5
40-50N	1	14	3	1	–	–	–	–	1	–	–	–	–	–
30-40N	26	96	46	14	5	1	–	–	4	3	1	–	–	–
20-30N	26	78	35	11	15	12	3	10	17	5	6	4	–	–
10-20N	39	90	19	8	12	10	7	8	33	2	4	5	4	2
0-10N	–	5	–	–	–	–	–	6	18	6	2	1	2	–

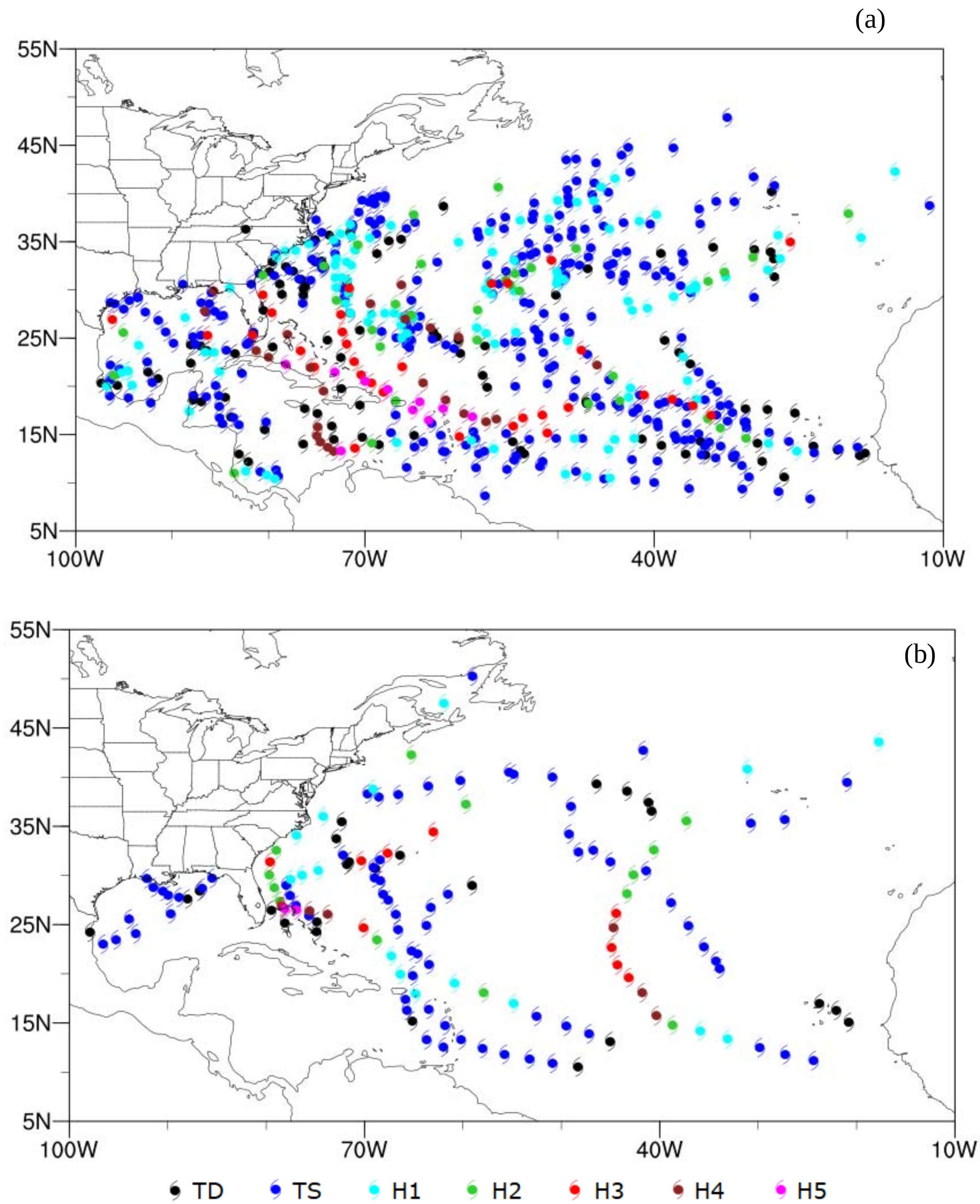

Figure 1: The geographic distribution of the tropical cyclone (TC) center covered by (a) the 577 cases during 2016-2018 and (b) 144 cases in 2019 over the Atlantic Ocean. Colors represent different TC intensities.

IV. Discussion

Previous studies show that the warm-core strength is better correlated with P_{min} than with V_{max} (Zhang & Chen, 2012; Zhu & Weng, 2013; Kieu et al., 2016; Gaona et al., 2017). Figure 2 shows the relationships between the TC intensity (V_{max} and P_{min}) and WC_{max} within 20 km of the storm centers for the 577 cases during 2016–2018. Considering the full TC intensity range, WC_{max} is well correlated with V_{max}, with a correlation coefficient of 0.786. The correlation with P_{min} is higher, with a correlation coefficient of -0.841. Using these correlation coefficients, estimated are V_{max} and P_{min} for the 144 TC cases in 2019. The MPE and RMSE for V_{max} are 39.04 and 42.70 mph, respectively, and the MPE and RMSE for P_{min} are 14.47 and 77.69 hPa, respectively.

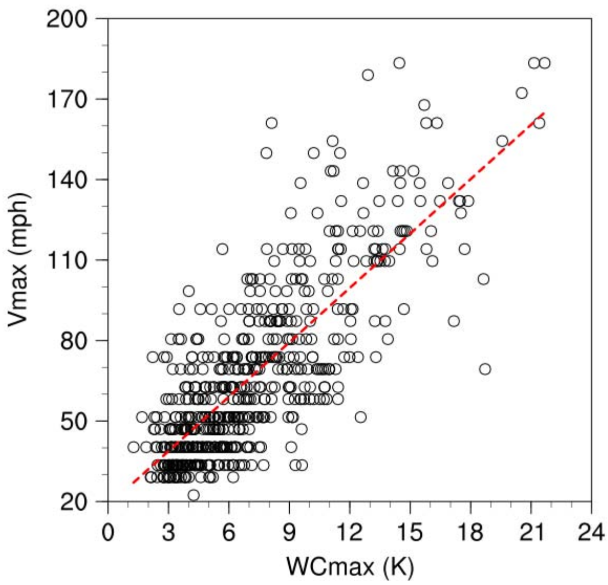

Figure 2: Scatterplots of WC_{max} versus V_{max} (left panel) and P_{min} (right panel) for the 577 TC cases during 2016-2018 shown in Fig. 1a. The linear regression fitting is indicated by the red dashed line. The Pearson correlation coefficients are 0.786 and -0.841, respectively.

The five ML models described in Section 2.2 (SVM, DT, AdaBoost, ADT, and RF) were constructed using only WC_{max} as the input. The 577 TC cases during 2016–2018 (Fig. 1a) were used in the training process, and the 144 TC cases in 2019 were used for validation. Table 2 lists the MPE and RMSE for each ML model. Compared to linear regression, the ML models all show better performances, shown by the decrease in MPE by ~60% for V_{max} and by ~50% for P_{min}. The RMSE also decreased by ~50% for V_{max} and by ~85% for P_{min}. The best performance occurred with the SVM model, where the MPE and RMSE for V_{max} are 14.62 and 19.91 mph, respectively, and the MPE and RMSE for P_{min} are 7.66 and 10.58 hPa, respectively.

Table 2: Estimates of V_{max} and P_{min} based on linear regression and SVM, DT, AdaBoost, ADT, and RF when the maximum warm-core strength is the only input to ML training.

ML Scheme	V_{max} (mph)		P_{min} (hPa)	
	MPE	RMSE	MPE	RMSE
Linear Regression	39.04	42.70	14.47	77.69
SVM	14.62	19.91	7.66	10.58
DT	15.00	20.61	8.12	10.85
Ada	15.89	20.79	9.62	12.09
ADT	16.49	21.27	8.94	11.24
RF	14.78	19.88	7.73	10.43

With the selection of those five ML schemes, experiments evaluating the ML model performance with seven different combinations of TC information were conducted (Table 3). The choices of TC information include: WCmax, Latitude (Lat), Longitude (Lon), day of year (DOY), and local time (LT). An average MPE of around 15.38 mph could be achieved if adding the information of latitude in ML training process (Exp. A). Among the five ML schemes, SVM produces the minimum MPE of 13.40 mph, with a minimum RMSE of 18.37 mph. The variation is within 4.2 mph for the MPE and within 3.39 mph for the RMSE. An average MPE of around 15.79 mph can be reached if adding the information of DOY in the ML training process (Exp. B). Again, SVM produces the minimum MPE of 14.19 mph, with a minimum RMSE of 19.92 mph. The variation is within 3.17 mph for the MPE and within 2.54 mph for the RMSE. With both Lat and DOY added into the training process, only the SVM performs better with the MPE decreased to 13.01 mph, and the RMSE decreased to 17.33 mph. Other ML schemes have larger MPEs and RMSEs. Since LT is derived from longitude through the relation LT=UTC+Lon/15, only adding LT or Lon is considered in Exp. D-G. Adding longitude (LT or Lon) information does not markedly improve the model performances, noting that the SVM still performs the best.

Table 3: Inputs to ML models

EXP	Inputs				
	WC_{max}	Lat	DOY	Lon	LT
A	✓	✓			
B	✓		✓		
C	✓	✓	✓		
D	✓	✓		✓	
E	✓	✓			✓
F	✓	✓	✓	✓	
G	✓	✓	✓		✓

For P_{min} (figures omitted), an average MPE of around 8.83 hPa can be achieved if adding the information of latitude in the ML training process (Exp. A). Among the five ML schemes, RF produces the minimum MPE of 7.75 hPa, with a minimum RMSE of 10.62 hPa. The variation is within 2.77 hPa for the MPE and within 2.24 hPa for the RMSE. An average MPE of around 8.85 hPa can be reached if adding the information of DOY in the ML training process (Exp. B). Again, the SVM produces the minimum MPE of 7.23 hPa, with a minimum RMSE of 9.88 hPa. The variation is within 3.80 hPa for the MPE and within 3.29 hPa for the RMSE. Adding both Lat and DOY into the training does not improve the performances. As with V_{max}, adding longitude (LT or Lon) information does not markedly improve the model performances, noting that the SVM still performs the best when adding latitude and DOY into the training process.

Since SVM and RF are the top two accurate models for all 7 different combinations of training variables (Fig. 3), The performance with different combinations of training variables for V_{max} and P_{min} are further examined (Fig.4). In general, all combination produces similar results, with small variations. The best estimation for V_{max} using SVM occurs when WC_{max}, Lat and DOY are used in training, while as for P_{min} occurs when WC_{max} and DOY are used in training. The best estimation of both V_{max} and P_{min} using RF occurs when WC_{max}, Lat and Lon are used in training. It's concluded that adding more TC information won't necessarily improve the estimation accuracy. The green box in Fig. 4 indicates the optimal combination option for SVM and RF. The performance of the optimal choice relative to the best track intensities is shown in Fig. 5, by stratifying the validation dataset of various intensities. Both models tend to have over-forecasts (MPE for V_{max} is positive, and MPE for P_{min} is negative) for tropical depressions and tropical storms, and under-forecasts (MPE for V_{max} is negative, and MPE for P_{min} is positive) for hurricanes. The mean V_{max} MPE for TD and TS is 10.77 mph for SVM, and 7.08 for RF, for Hurricane is -4.72 mph for SVM and -7.96 mph. The mean P_{min} MPE for TD and TS is -3.47 hPa for SVM, and -4.80 hPa for RF, for Hurricane is 4.79 hPa for SVM and 3.98 hPa. The smaller sample size of hurricane cases may contribute to the larger variation in underestimation situation for hurricanes. A future modification to address this issue will be to randomly drop out the samples with tropical storm intensities in the training data for reducing the overall sampling bias.

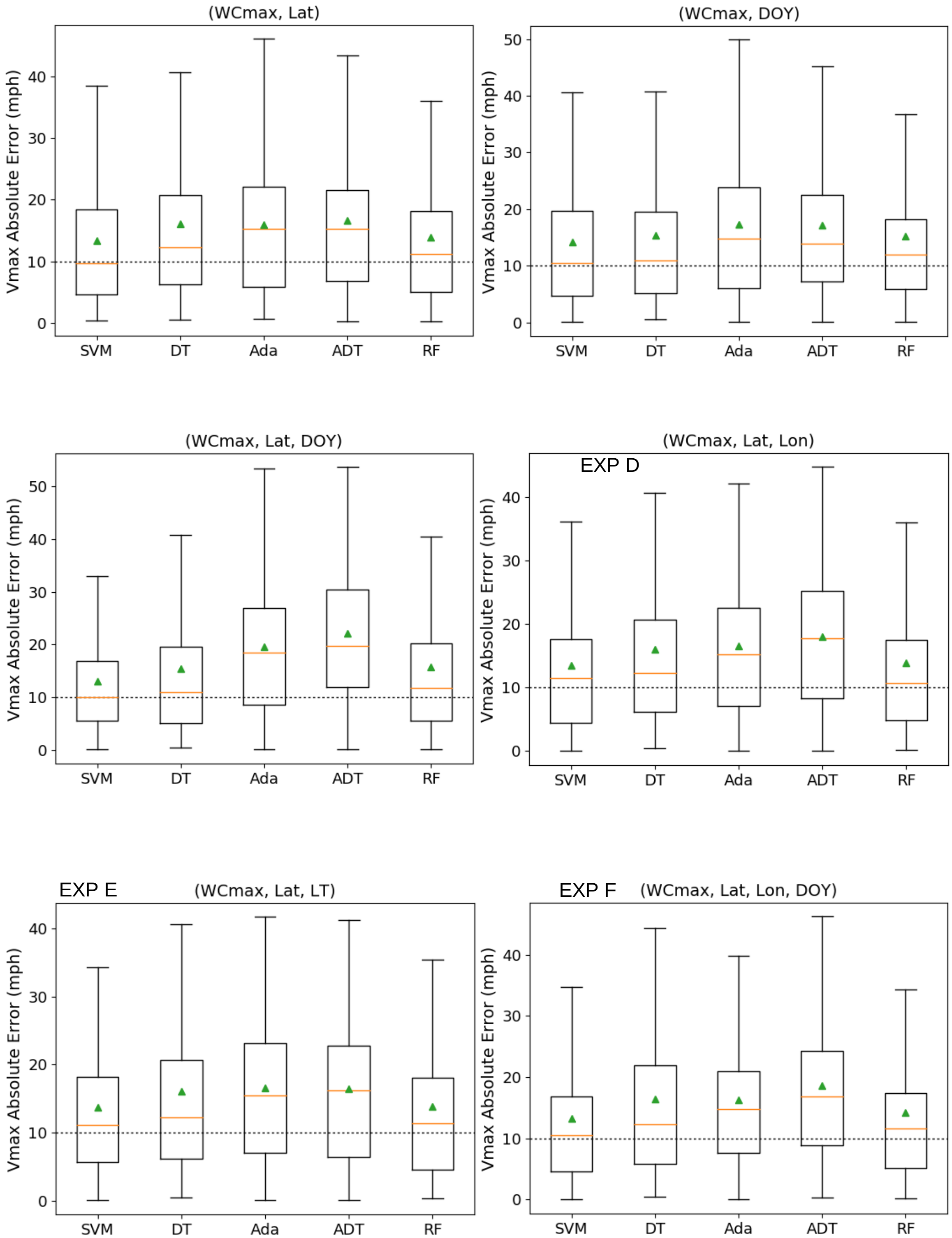
(WCmax, Lat)
(WCmax, DOY)
(WCmax, Lat, DOY)
EXP D
(WCmax, Lat, Lon)
EXP E
(WCmax, Lat, LT)
EXP F
(WCmax, Lat, Lon, DOY)
Vmax Absolute Error (mph)
SVM
DT
Ada
ADT
RF

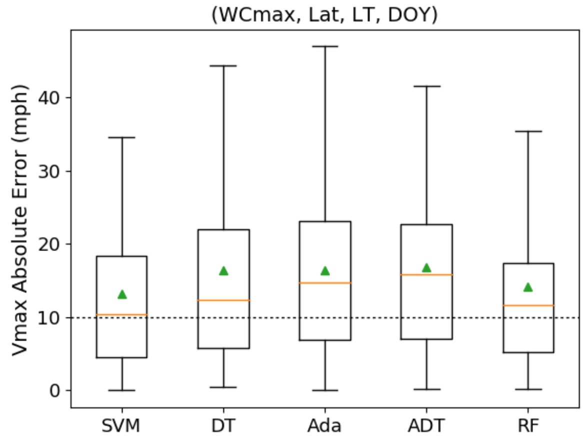

Figure 3: Boxplots of the absolute V_{max} errors relative to the best track intensity for SVM, DT, Ada, ADT, and RF scheme in a comparison with n=144 samples from the TC cases in 2019. On each box, the median (orange line), 25th percentile, and 75 percentile are indicated; the whiskers extend to the 5th and 95th percentiles; the green triangle indicates the mean MPE. The TC information used in the training of ML schemes is listed on top of each panel.

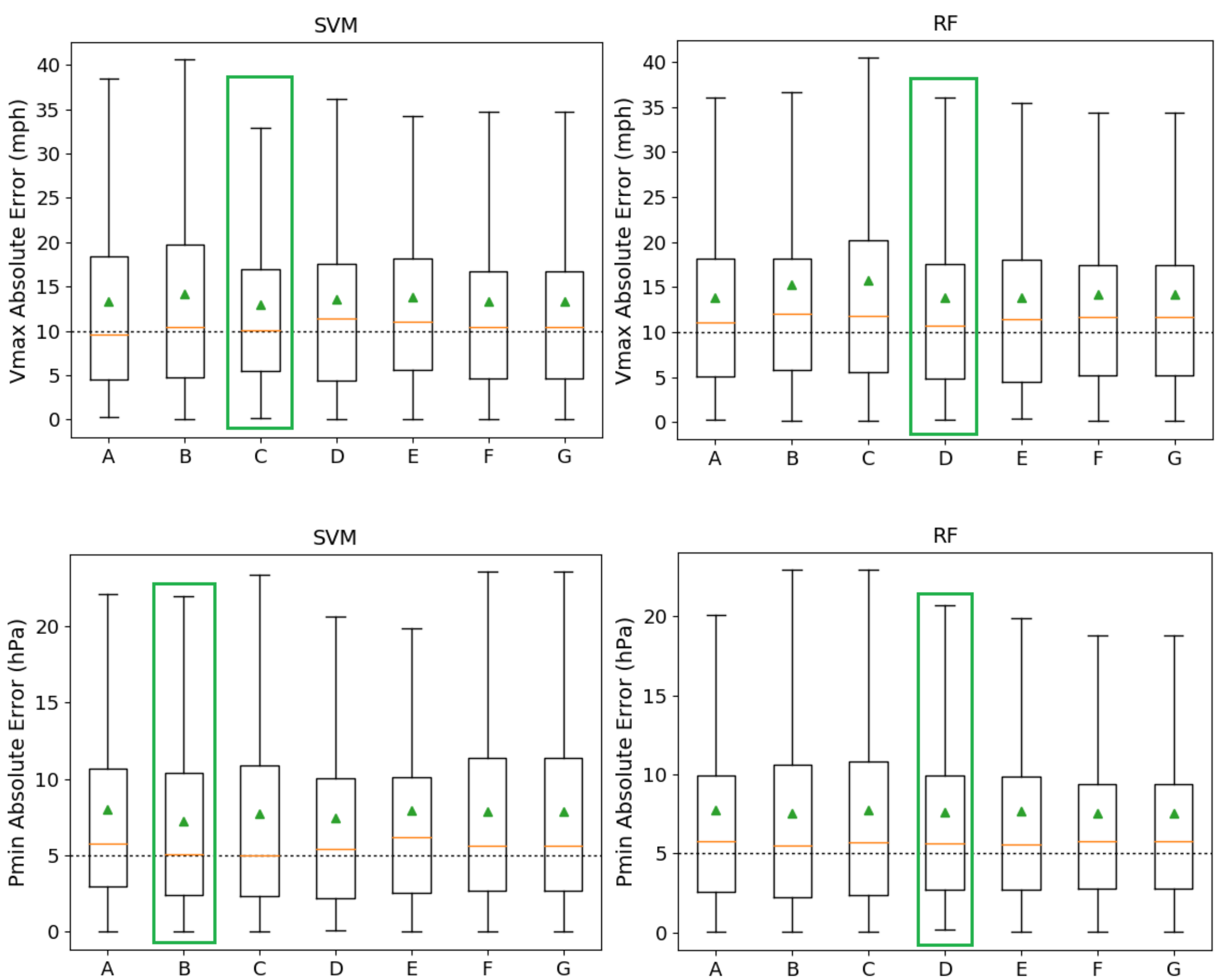

Figure 4: Boxplots of (a-b): the absolute V_{max} errors and (c-d): the absolute P_{min} errors relative to the best track intensity for SVM (left panels) and Random Forest model (right panels).

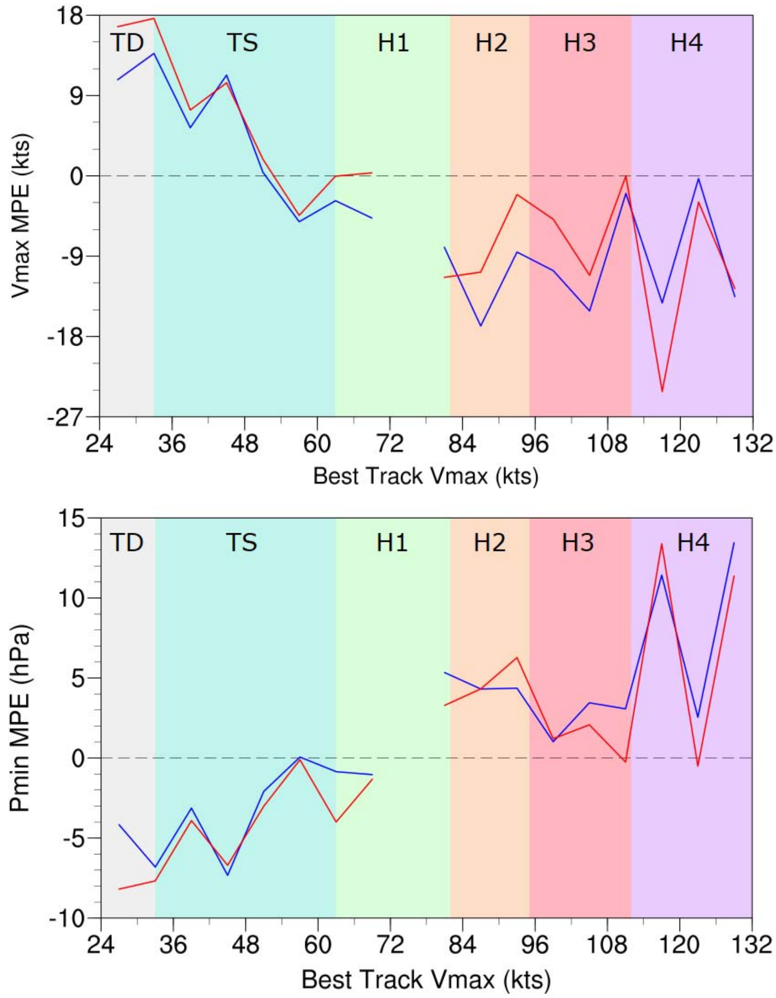

Figure 5: MPE of V_{max} (upper) and P_{min} (lower) according to best track V_{max} from SVM (blue) and RF models (red). The combinations of TC information used in this figure are corresponding to the green box in Fig. 4.

V. Summary and Conclusions

The warm-core structure is an important parameter for monitoring the TC intensity, studying TC inner-core dynamics, and establishing the initial vortices for TC simulation and prediction. Traditionally, WC_{max} is considered to be directly related to the intensity of a TC. From the 577 Atlantic TCs observed by the S-NPP ATMS during the period 2016–2018, the correlation coefficients between WC_{max} and the V_{max} and P_{min} of TCs are 0.786 and -0.841, respectively. The MPE and RMSE for V_{max} are 39.04 and 42.70 mph, respectively, and the MPE and RMSE for P_{min} are 14.47 and 77.69 hPa, respectively. ML estimation results indicate that the overall MPE for V_{max} is 15.36 mph, with more than a 60% decrease, and for P_{min} is 8.41 hPa, with more than a 50% decrease.

The present study also developed several ML models using different combinations of TC information (including latitude, longitude, DOY, and LT) as inputs to the training process for hurricane intensity estimation. The best estimation of V_{max} from the SVM model occurs when the training process uses WC_{max}, Lat, and DOY. The MPE and RMSE are 13.01 mph and 17.33 mph, respectively. The best estimation of P_{min} from the SVM model occurs when the training process uses WC_{max} and DOY. The MPE and RMSE are 7.23 hPa and 9.88 hPa, respectively.

The results from this study show that ML algorithms can capture the complex relationship between TC information and hurricane intensity, thereby avoiding complex intermediate processing. This can feasibly simplify and improve hurricane intensity estimation. Future studies will modify the retrieval of atmospheric temperature from the ATMS by considering scattering effects using ML methods and will extend the present study to the Pacific Ocean to develop an accurate estimation of typhoon intensity using the maximum warm-core intensity (WC_{warm}) and other TC information.

Acknowledgments

This work was supported by NOAA grant NA19NES4320002 (Cooperative Institute for Satellite

Earth System Studies-CISESS) at the Earth System Science Interdisciplinary Center (ESSIC), University of Maryland (UMD).The data sets used in this paper are freely available online. S-NPP ATMS TDR data can be obtained from NOAA/CLASS (https://www.bou.class.noaa.gov/saa/products/search?sub_id=0&datatype_family=ATMS_TDR&submit.x=35&submit.y=11), and the hurricane best track information from the National Hurricane Center (https://www.nhc.noaa.gov/data/hurdat/hurdat2-1851-2018-120319.txt).

References Références Referencias

1. Brown, S., B. Lambrigtsen, B. Lim, & T. Gaier (2017), Demonstrating the impact of rapid repeat passive microwave observations from the global hawk: Implications for future SmallSat or GEO missions. Proceedings of 2017 IEEE International Geoscience and Remote Sensing Symposium, Fort Worth, TX, USA, 5938–5941. doi: 10.1109/IGARSS.2017.8128361
2. Dolling, K. & G. M. Barnes (2012), Warm-core formation in Tropical Storm Humberto (2001). Monthly Weather Review, 140, 1177–1190. doi:10.1175/MWR-D-11-00183.1
3. ——, & G. M. Barnes (2014), The evolution of Hurricane Humberto (2001). Journal of Atmospheric Sciences, 71, 1276–1291. doi: 10.1175/ JAS-D-13-0164.1
4. Durden, S. L., 2013: Observed tropical cyclone eye thermal anomaly profiles extending above 300hPa. Monthly Weather Review, 141, 4256–4268, doi:10.1175/MWR-D-13-00021.1.
5. Galarneau, T. J., Jr., C. A. Davis, & M. A. Shapiro (2013), Intensification of Hurricane Sandy (2012) through extratropical warm core seclusion. Monthly Weather Review, 141, 4296–4321. doi:10.1175/MWR-D-13-00181.1
6. Gaona,M.F. R., A. Overeem, A. M. Brasjen, J. F. Meirink, H. Leijnse,&R. Uijlenhoet (2017), Evaluation of rainfall products derived from satellites and microwave links for the Netherlands. IEEE Transanctionon Geoscience and Remote Sensing, 55, 6849–6859. doi:10.1109/TGRS.2017.2735439
7. Goldberg, M.D. (1999), Generation of retrieval products from AMSU-A: Methodology and validation. 10 th Int. ATOVS Study Conference, Boulder, CO, 219-229.
8. Han, Y., & F. Weng (2018), Remote sensing of tropical cyclone thermal structure from satellite microwave sounding instruments: Impacts of optimal channel selection on retrievals. Journal of Meteorological Research, 32(5), 804–818. doi: 10.1007/s13351-018-8005-x
9. Halverson, J. B., J. Simpson, G. Heymsfield, H. Pierce, T. Hock, & L. Ritchie (2006), Warm core structure of Hurricane Erin diagnosed from high altitude dropsondes during CAMEX-4. Journal of Atmospheric Sciences, 63, 309–324. doi:10.1175/JAS3596.1
10. Hawkins, H. F., & D. A. Rubsam (1968), Hurricane Hilda, 1964. Part II: Structure and budgets of the hurricane core on 1 October 1964. Monthly Weather Review, 96, 617–636. doi:10.1175/ 1520-0493(1968)096,0617:HH.2.0.CO;2
11. & S. M. Imbembo (1976), The structure of a small, intense Hurricane-Inez 1966. Monthly Weather Review, 104, 418–442. doi:10.1175/1520-0493(1976)104,0418:TSOASI.2.0.CO;2
12. Hu, H., F. Weng, Y. Han, & Y. Duan (2019), Remote sensing of tropical cyclone thermal structure from satellite microwave sounding instruments: impacts of background profiles on retrievals. Journal of Meteorological Research, 33(1), 89–103. doi:10.1007/s13351-019-8094-1
13. Kidder, S. Q., W. M. Gray, & T. H. Vonder Haar (1978), Estimating tropical cyclone central pressure and outer winds from satellite microwave data. Monthly Weather Review, 106, 1458–1464. doi:10.1175/1520-0493(1978)106<1458:ETCCPA>2.0.CO;2
14. ——, ——, & —— (1980), Tropical cyclone outer surface winds derived from satellite microwave data. Monthly Weather Review, 108, 144–152. doi:10.1175/1520-0493(1980)108 <0144:TCOSWD>2.0.CO;2
15. ——, M. D. Goldberg, R. M. Zehr, M. DeMaria, J. F. W. Purdom, C. S. Velden, N. C. Grody, & S. J. Kusselson (2000), Satellite analysis of tropical cyclones using the Advanced Microwave Sounding Unit (AMSU). Bulletin of American Meteorological Society, 81, 1241–1260. doi:10.1175/1520-0477(2000)081<1241:SAOTCU>2.3.CO;2
16. Kieu, C., V. Tallapragada, D.-L. Zhang, & Z. Moon(2016), On the development of double warm cores in intense tropical cyclones. Journal of Atmospheric Sciences, 73, 4487–4506, doi:10.1175/JAS-D-16-0015.1.
17. Knaff, J. A., S. A. Seseske, M. DeMaria, & J. L. Demuth (2004), On the fluences of vertical wind shear on symmetric tropical cyclone structure derived from AMSU. Monthly Weather Review, 132, 2503–2510. doi:10.1175/1520-0493(2004)132,2503:OTIOVW.2.0.CO;2
18. La Seur, N. E., & H. F. Hawkins (1963), An analysis of Hurricane Cleo (1958) based on data from research reconnaissance aircraft. Monthly Weather Review, 91, 694–709. doi:10.1175/1520-0493(1963)091,0694:AAOHCB.2.3.CO;2
19. Lin, L, & F. Weng (2018), Estimation of hurricane maximum wind speed using temperature anomaly derived from advanced technology microwave sounder. IEEE Geoscience and Remote Sensing

Letters, 15(5), 639–643. doi:10.1109/LGRS.2018. 2807763.

20. Munsell, E. B., F. Zhang, S. A. Braun, J. A. Sippel, & A. C. Didlake (2018), The inner-core temperature structure of Hurricane Edouard (2014): Observations and ensemble variability. Monthly Weather Review, 146, 135–155. doi:10.1175/ MWR-D-17-0095.1.
21. Stern, D. P., & F. Zhang (2016), The warm-core structure of Hurricane Earl (2010). Journal of Atmospheric Sciences, 73, 3305–3328. doi:10.1175/ JAS-D-15-0328.1.
22. Tian, X., & X. Zou (2016), ATMS- and AMSU-A-derived hurricane warm core structuresusing a modified retrieval algorithm. Journal of Geophysical Research: Atmosphere, 121, 12630–12646. doi:10.1002/2016JD025042.
23. Velden, C. S., & W. L. Smith (1983), Monitoring tropical cyclone evolution with NOAA satellite microwave observations. Journal of Climate and Applied Meteorology, 22, 714–724. doi:1520-0450(1983)022<0714:MTCEWN>2.0.CO;2.
24. ——, (1989), Observational analyses of North Atlantic tropical cyclones from NOAA polar-orbiting satellite microwave data. Journal of Applied Meteorology, 28, 59–70. doi:10.1175/1520-0450(1989)028<0059:OAONAT>2.0.CO;2.
25. ——, B. M. Goodman, & R. T. Merrill (1991), Western North Pacific tropical cyclone intensity estimation from NOAA polar-orbiting satellite microwave data. Monthly Weather Review, 119, 159–168. doi:10.1175/1520-0493(1991)119<0159: WNPTCI>2.0.CO;2.
26. Wang, X., & H. Jiang (2019). A 13-Year Global Climatology of Tropical Cyclone Warm-Core Structures from AIRS Data. Monthly Weather Review, 147(3), 773–790. doi:10.1175/MWR-D-18-0276.1.
27. Wang, Z., M. T. Montgomery, & T. J. Dunkerton (2010), Genesis of preHurricane Felix (2007). Part II: Warm core formation, precipitation evolution, and predictability. Journal of Atmospheric Sciences, 67, 1730–1744. doi:10.1175/2010JAS3435.1.
28. Weng, F., L. Zhao, R. Ferraro, G. Poe, X. Li, & N. Grody (2003), Advanced microwave sounding unit cloud and precipitation algorithms. Radio Science, 38(4), 8086-8096. doi:10.1029/2002RS002679.
29. ——, X. Zou, X. Wang, S. Yang, & M. Goldberg (2012), Introduction to Suomi NPP ATMS for NWP and tropical cyclone applications. Journal of Geophysical Research, 117(D19112), 1–14. doi:10.1029/2012JD018144.
30. Zhang, D.-L., & H. Chen (2012), Importance of the upper-level warm core in the rapid intensification of a tropical cyclone. Geophysical Research Letter, 39(L02806), 1–6. doi:10.1029/2011GL050578.
31. Zhang, K., L. Zhou, M. Goldberg, X. Liu, W. Wolf, C. Tian, & Q. Liu (2017), A methodology to adjust ATMS observations for limb effect and its applications. Journal of Geophysical Research: Atmosphere, 122 (21), 11,347–11,356. doi:10.1002/ 2017JD026820.
32. Zhu, T., D.-L. Zhang, & F. Weng (2002), Impact of the Advanced Microwave Sounding Unit measurements on hurricane prediction. Monthly Weather Review, 130, 2416–2432. doi:10.1175/1520-0493(2002)130<2416:IOTAMS>2.0.CO;2.
33. ——, & F. Weng (2013), Hurricane Sandy warm-core structure observed from Advanced Technology Microwave Sounder. Geophysical Research Letter, 40, 3325–3330. doi:10.1002/grl.50626.